Article

Liquid Crystal Behavior of Single-Walled Carbon Nanotubes Dispersed in Biological Hyaluronic Acid Solutions

Simon E. Moulton, Maryse Maugey, Philippe Poulin, and Gordon G. Wallace

J. Am. Chem. Soc., **2007**, 129 (30), 9452-9457• DOI: 10.1021/ja072160h • Publication Date (Web): 10 July 2007

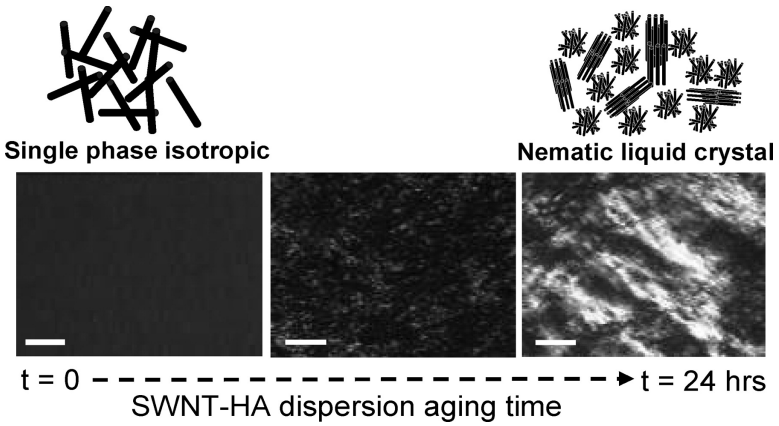

More About This Article

Additional resources and features associated with this article are available within the HTML version:

- Supporting Information
- Links to the 7 articles that cite this article, as of the time of this article download
- Access to high resolution figures
- Links to articles and content related to this article
- Copyright permission to reproduce figures and/or text from this article

View the Full Text HTML

J|A|C|S
ARTICLES
Published on Web 07/10/2007

Liquid Crystal Behavior of Single-Walled Carbon Nanotubes Dispersed in Biological Hyaluronic Acid Solutions

Simon E. Moulton,[†] Maryse Maugey,[‡] Philippe Poulin,[‡] and Gordon G. Wallace*,[†]

Contribution from the ARC Centre of Excellence for Electromaterials Science, Intelligent Polymer Research Institute, University of Wollongong, New South Wales, Australia, and Centre de Recherches Paul Pascal, Universitle Bordeaux I, UPR CNRS 8641, France

Received March 27, 2007; E-mail: gwallace@uow.edu.au

Abstract: We report the spontaneous liquid crystal phase separation of nanotubes (single-walled carbon nanotubes, SWNTs) stabilized in aqueous biological (hyaluronic acid, HA) solutions. Sonication of SWNTs in solutions of HA produced well-dispersed single-phase isotropic dispersions which, over time, phase separated into dispersions containing birefringent nematic domains in equilibrium with an isotropic phase. The time required for phase separation to occur was shown to depend on the concentration of SWNT and HA, with the attractive interactions between the SWNT and HA shifting the onset of the phase separation toward lower concentration. This phase separation is accompanied by an increase in the dispersion viscosity with this increase qualitatively matching the degree of phase separation. The formation of ordered phases in biological media can offer wide opportunities for processing conducting biomaterials with aligned and oriented domains.

It is expected that the integration of carbon nanotubes (CNTs) into biomaterials will provide enhanced properties and performance.[1−4] The integration of CNTs into materials should be facilitated by functionalization with biological molecules such as proteins or oligosaccharides.[5−10] Such functionalization can be achieved using either a covalent[11] or noncovalent[12] approach. The functionalization plays two roles in that it provides a means to effectively disperse the CNTs in a medium that is suitable for processing biomaterials and the biomolecule then plays a role in providing an appropriate interface to the biological environment of interest. Combining the unique electronic properties of CNTs with the biomolecular recognition capabilities induced by such functionalization also provides a platform for miniaturized biological electronics and optical devices including sensors.[13]

The phase behavior of CNT dispersions is of primary importance as the starting point for their further processing into a number of forms such as films and composites. A number of studies have been performed investigating the phase behavior of CNTs dispersions using diamines,[14] surfactants,[15] DNA,[16] and acids[17−19] Ordered phases, in contrast to those that are isotropic in nature, offer wide opportunities for processing materials with aligned and oriented domains, an important factor considering the strong anisotropic properties of CNTs.[16] It is therefore, critical to study the interaction between CNTs and biomolecules in solution and in particular to determine the possibility of forming ordered phases due to the presence of the biomolecules. In addition, major classes of biological compounds including lipids, proteins, carbohydrates, and nucleic acids all have been found to exist in various liquid crystalline phase in vivo as well as in vitro under well-defined conditions.[20] Their liquid crystalline structure is envisaged to have a very important role in their biological functions and self-assembly processes.[20] Optimization of these dispersed assemblies under various conditions will then lead to CNT−biomolecule structures in the form of films, fibers, or coatings with controllable mechanical and/or electrical properties.

[†] University of Wollongong.
[‡] Universitle Bordeaux I.

(1) Erlanger, B. F.; Chen, B.; Zhu, M.; Brus, L. E. *Nano Lett.* **2001**, *1*, 465.
(2) Taton, T. A.; Mirkin, C. A.; Letsinger, R. L. *Science* **2000**, *289*, 1757.
(3) Harrison, B. S.; Atala, A. *Biomaterials* **2007**, *28*, 344.
(4) Smart, S. K.; Cassady, A. I.; Lu, G. Q.; Martin, D. J. *Carbon* **2006**, *44*, 1034.
(5) Baker, S. E.; Cai, W.; Lasseter, T. L.; Weidkamp, K. P.; Hamers, R. J. *Nano Lett.* **2002**, *2*, 1413.
(6) Guo, Z. J.; Sadler, P. J.; Tsang, S. C. *Adv. Mater.* **1998**, *10*, 701.
(7) Fu, K.; Huang, W.; Lin, Y.; Zhang, D.; Hanks, T. W.; Rao, A. M.; Sun, Y. P. *J. Nanosci. Nanotechnol.* **2002**, *2*, 457.
(8) Pantarotto, D.; Partidos, C. D.; Graff, R.; Hoebeke, J.; Briand, J. P.; Prato, M.; Bianco, A. *J. Am. Chem. Soc.* **2003**, *125*, 6160.
(9) Chen, R. J.; Zhang, Y. G.; Wang, D.; Dai, H. J. *J. Am. Chem. Soc.* **2001**, *123*, 3838.
(10) Balavoine, F.; Schultz, P.; Richard, C.; Mallouh, V.; Ebbesen, T. W.; Mioskowski, C. *Angew. Chem., Int. Ed.* **1999**, *38*, 1912.
(11) Jiang, K.; Schadler, L. S.; Siegel, R. W.; Zhang, X.; Zhang, H.; Terrones, M. *J. Mater. Chem.* **2004**, *14*, 37.
(12) Karajanagi, S. S.; Yang, H. C.; Asuri, P.; Sellitto, E.; Dordick, J. S.; Kane, R. S. *Langmuir* **2006**, *22*, 1392.
(13) Shim, M.; Kam, N. W. S.; Chen, R. J.; Li, Y.; Dai, H. J. *Nano Lett.* **2002**, *2*, 285.
(14) Brown, J. M.; Anderson, D. P.; Justice, R. S.; Lafdi, K.; Belfor, M.; Strong, K. L.; Schaefer, D. W. *Polymer* **2005**, *46*, 10854.
(15) Weiss, V.; Thiruvengadathan, R.; Regev, O. *Langmuir* **2006**, *22*, 854.
(16) Badaire, S.; Zakri, C.; Maugey, M.; Derre, A.; Barisci, J. N.; Wallace, G. G.; Poulin, P. *Adv. Mater.* **2005**, *17*, 1673.
(17) Song, W.; Kinloch, I. A.; Windle, A. H. *Science* **2003**, *302*, 1363.
(18) Rai, P. K.; Pinnick, R. A.; Parra-Vasquez, A. N. G.; Davis, V. A.; Schmidt, H. K.; Hauge, R. H.; Smalley, R. E.; Pasquali, M. *J. Am. Chem. Soc.* **2006**, *128*, 591.
(19) Davis, V. A.; Ericson, L. M.; Parra-Vasquez, A. N. G.; Fan, H.; Wang, Y.; Prieto, V.; Longoria, J. A.; Ramesh, S.; Saini, R. K.; Kittrell, C.; Billups, W. E.; Adams, W. W.; Hauge, R. H.; Smalley, R. E.; Pasquali, M. *Macromolecules* **2004**, *37*, 154.
(20) Rizvi, T. Z. *J. Mol. Liq.* **2003**, *106*, 43.

 10.1021/ja072160h CCC: $37.00

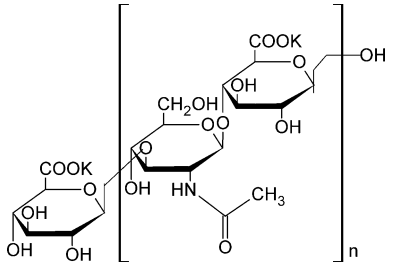

Figure 1. Structure of hyaluronic acid (HA).

Hyaluronic acid (HA) is a glucosaminoglycan (Figure 1) distributed widely throughout connective, epithelial, and neural tissue. It is one of the chief components of the extracellular matrix and contributes significantly to cell proliferation and migration. It is therefore an important molecule to investigate in relation to forming biologically compatible materials based on CNTs.

In this work we investigate the properties of SWNTs dispersed in solutions of HA using transmission polarized microscopy, dynamic light scattering, and rheology. The results demonstrate the remarkable dispersive properties of HA and the slow but spontaneous phase transition involving formation of a nematic liquid crystal phase due to organization of the CNTs in "solution". In addition, the nanotubes are used as support platforms to facilitate ordered HA-based material.

Single-walled carbon nanotubes (SWNTs) made by the HiPco process were obtained from Carbon Nanotechnologies, Inc., (batch no. P0279). Hyaluronic acid HA was purchased from Sigma Aldrich and used as received. All the sonication experiments are performed in a dispersion (2 mL) containing various SWNT and HA concentrations (wt %) in Milli-Q water. The dispersions are obtained using a Branson homogenizer, Sonifier model S-250A equipped with a 13 mm step disruptor horn and a 3 mm tapered microtip, operating at a 20 kHz frequency and 40 W. All dispersions were sonicated for 60 min in a water−ice bath to prevent the suspension from overheating. Homogeneity and birefringence of the dispersion were checked using an Olympus BH-2 microscope in transmission mode between crossed polarizers. The dynamic light scattering (DLS) experiments[21] are performed at 20 °C on SWNT−HA suspensions, by diluting the various wt % dispersions with Milli-Q water filtered two times on 0.22 μm membranes. These experiments are carried out using a Coherent Innova 90 krypton ion laser operating at $\lambda = 647.1$ nm and $P_{\text{laser}} = 70$ mW and a Brookhaven BI-9000AT digital autocorrelator to compute the scattered photons time autocorrelation function (ACF). For the light-scattering experiments it was necessary to allow the samples to equilibrate for 2 weeks before any measurement was made, to allow any large particles that may have been present to sediment. Viscosity measurements were made using an Anton Paar (Germany) Physica MCR 301 rheometer utilizing a 20 mm parallel flat plate spindle arrangement at 25 °C.

Transmission electron microscopy (TEM) images were recorded using a Philips CM200 HiRes TEM utilizing an accelerating voltage of 200 keV. A 30 μL droplet of diluted (500 times) SWNT dispersion was cast onto a lacey hole carbon copper TEM grid and allowed to dry at room temperature prior to TEM imaging.

(21) See the Supporting Information for a brief description of the DLS method.

The phase diagram shown in Figure 2a was constructed from observations made using the optical microscope immediately after sonication was completed. With the use of a wide range of SWNT and HA concentrations it was possible to form solutions where the nanotube bundles are homogenously dispersed forming a single-phase isotropic dispersion (hereafter only referred to as isotropic). The birefringence of the isotropic dispersions was also imaged using the microscope in transmission mode between crossed polarizers. The optical and cross-polarized images of the isotropic dispersion (Figure 2b) shows a featureless image characteristic of well-dispersed SWNTs. The inset image is the cross-polarized image which exhibits no birefringent domains.

Poorly dispersed solutions result when the SWNT-HA concentration ratio is not adjusted correctly (Figure 2c). The optical image in Figure 2c shows large aggregates of nondispersed SWNTs that exhibit no birefringence. These poorly dispersed systems were observed when the HA concentration was not sufficient to overcome the strong intertube van der Waals attraction of the SWNTs (e.g., 0.7 wt % SWNT/0.2 wt % HA). This has also been observed in SWNT−DNA systems[16] and indicates that a well-defined minimum amount of HA has to be adsorbed onto the nanotubes in order for an isotropic dispersion to form. Poor dispersions also occur when the concentration of HA is too great as seen for the 0.5 wt % SWNT/2 wt % HA dispersion. In this case the viscosity of the HA solution is too great preventing adequate dispersing of the SWNTs. These results indicate the choice of SWNT and HA concentration is critical in forming homogeneous isotropic dispersions. The interaction between the SWNTs and HA is thought to be noncovalent in nature with the HA molecule wrapping itself around the SWNTs in solution during the sonication process. This wrapping phenomenon has been used by others to explain the dissolution of CNTs in solutions containing large polymer molecules.[22,23]

The efficient stabilization at low SWNT-HA concentrations (0.65:0.3 wt %, ratio of 1:0.47) is testimony to the remarkable dispersive properties of HA, with the lowest amount of HA required to obtain a stable isotropic SWNT dispersion being 0.1 wt %. In comparison to several other dispersing agents this ratio is much lower. Grossiord[24] et al. showed, using a variety of methods, that the minimum amount of sodium dodecyl sulfate (SDS) required to obtain stable SWNT dispersions was 1.7 times the amount of SWNTs (1:1.7), whereas others[25] have shown the optimum ratio for sodium dodecylbenzene sulfonate (NaDDBS) to be 1:10. Researchers have reported that to obtain stable SWNT dispersions using biomolecules as the dispersing agent it was necessary to employ a ratio of 1:1[26] or 1:2[27] for DNA and 1:2 for chitosan.[26]

Typically for rigid polymer or rodlike particle solutions a phase change, from isotropic to biphasic, only occurs when the

(22) Coleman, J. N.; Dalton, A. B.; Curran, S.; Rubio, A.; Davey, A. P.; Drury, A.; McCarthy, B.; Lahr, B.; Ajayan, P. M.; Roth, S.; Barklie, R. C.; Blau, W. J. *Adv. Mater.* **2000**, *12*, 213.
(23) Curran, S. A.; Ajayan, P. M.; Blau, W. J.; Carroll, D. L.; Coleman, J. N.; Dalton, A. B.; Davey, A. P.; Drury, A.; McCarthy, B.; Maier, S.; Strevens, A. *Adv. Mater.* **1998**, *10*, 1091.
(24) Grossiord, N.; van der School, P.; Meuldijk, J.; Koning, C. E. *Langmuir* **2007**, *23*, 3646.
(25) Islam, M. F.; Rojas, E.; Bergey, D. M.; Johnson, A. T.; Yodh, A. G. *Nano Lett.* **2003**, *3*, 2.
(26) Lynam, C.; Moulton, S. E.; Wallace, G. G. *Adv. Mater.* **2007**, *19*, 1244.
(27) Cathcart, H.; Quinn, S.; Nicolosi, V.; Kelly, J. M.; Blau, W. J.; Coleman, J. N. *J. Phys. Chem. C* **2007**, *11*, 66.

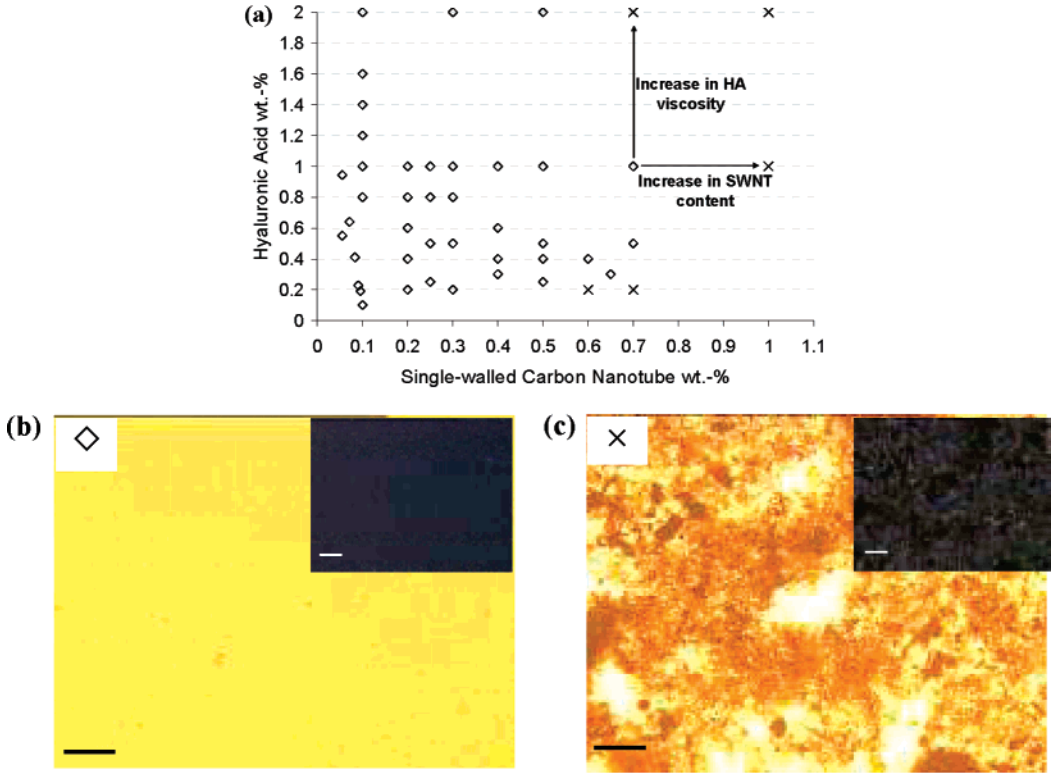

Figure 2. Phase diagram of HA-stabilized SWNTs in water (a) and optical (b and c) images of the solutions taken immediately after sonication. The ◊ symbol represents an isotropic dispersion, whereas × represents a poorly dispersed solution. The insets of each optical image are the corresponding cross-polarized light image (scale bar: 100 μm).

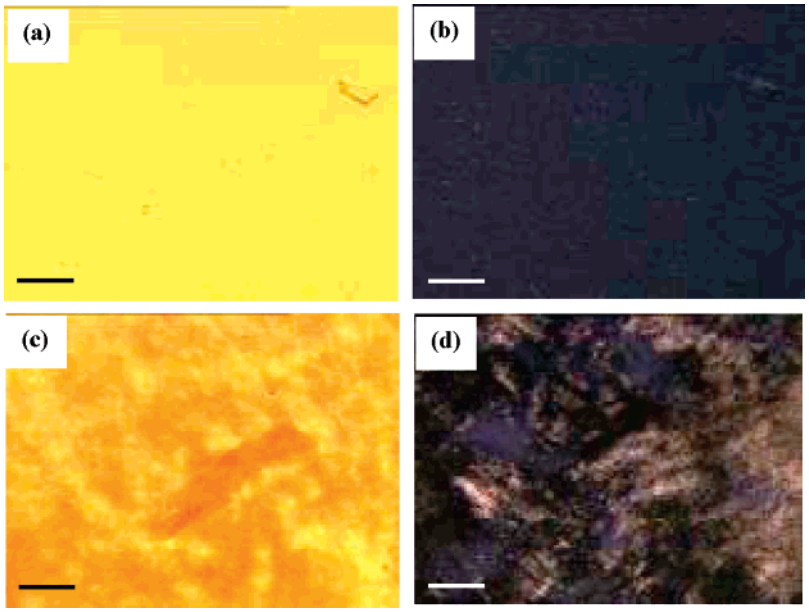

Figure 3. Optical (a and c) and crossed polarized (b and d) images of 0.5:1.0 wt % SWNT−HA dispersion taken immediately after sonication (a and b) and 24 h after sonication (c and d) (scale bar: 100 μm). The dispersions were sonicated for 60 min with a small (~25μL) droplet of the resulting dispersion placed between two glass coverslips followed by optical image analysis. The dispersion was set aside in an airtight sealed vial for 24 h before repeating the optical image analysis.

rigid polymer or rodlike particle concentration is increased. The biphasic system includes a birefringent nematic liquid crystal in equilibrium with an isotropic phase. Homogeneity and birefringence of the SWNT−HA dispersions was checked using the microscope in transmission mode between crossed polarizers 24 h after sonication (Figure 3). The images in Figure 3 show the phase properties of the SWNT−HA dispersion changing from isotropic to biphasic. Images a and b in Figure 3 show an isotropic dispersion which exhibits no birefringence, while 24 h later (images c and d in Figure 3) the same dispersion clearly exhibits a biphasic nature that exhibits strong birefringence. These birefringent domains coalesce when they touch each other demonstrating that they still are liquid in nature. This feature has also been observed for SWNT−DNA systems at much higher concentrations and has been described as nematic domains in equilibrium with an isotropic phase.[16] The disper-

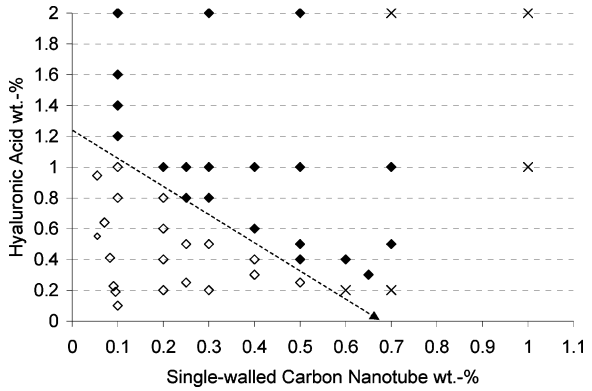

Figure 4. Phase diagram of HA-stabilized SWNTs in water. The phase diagram was constructed using optical image analysis of SWNT−HA dispersions 24 h after sonication. The ◊ symbol represents the dispersions that exhibit an isotropic behavior, whereas ♦ represents the dispersions that have phase separated into a biphasic system. The poorly dispersed solutions are represented by the × symbol. The dashed line represents the domain boundary between isotropic and biphasic dispersion.

sions that remained isotropic showed no evidence of SWNT precipitation 6 months after dispersion formation. The phase-separated dispersions also showed the same stability with no SWNT aggregations being observed under optical microscopy analysis.

Rai et al.[18] and Davis et al.[19] have elegantly shown that SWNTs in superacids roughly parallel the phase behavior of rodlike polymers. With increasing concentration, such systems exhibit transitions from dilute to semidiluted solutions. At even higher concentrations, the systems phase separate into a liquid crystalline nematic phase in equilibrium with an isotropic phase. The formation of the nematic phase can be understood in systems of hard rods by just considering translational and rotational entropies.[1] In the absence of interactions other than hard core, the transition occurs at a volume fraction of $3.3D/L$, where D and L, respectively, are the diameter and length of the rods.[28] However, attractive interactions can shift the onset of the phase separation toward lower concentration.[29,30] Nematic nanotube phases reported so far have only been observed upon increasing concentration. The transition from isotropic to biphasic system for the SWNT−HA dispersion described here is a spontaneous process that occurs as time elapses without any further addition of SWNTs. The vials containing the dispersions were sealed with an airtight snap lock lid between optical measurements to avoid unwanted evaporation of the solvent, which would result in an increase in SWNT and HA concentration. To our knowledge this is the first example of slow but still spontaneous phase transitions from isotropic to a biphasic system for CNT systems. This spontaneous phase transition is dependent on the ratio of SWNT−HA concentration which is highlighted in the phase diagram presented in Figure 4. This phase diagram was constructed using optical and birefringence measurements taken 24 h after sonication. There is a distinct phase boundary separating the isotropic and biphasic region (indicated by the dashed arrow in Figure 4). Above this phase boundary the isotropic dispersions spontaneously change to a biphasic system within 24 h of sonication. No further

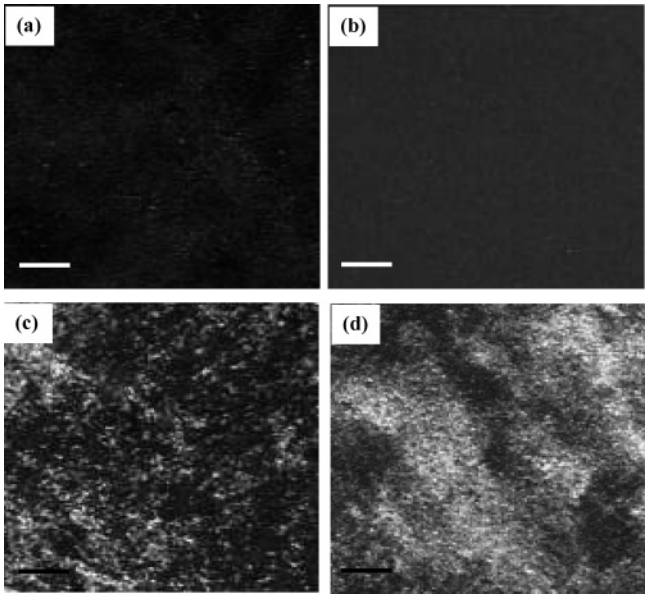

Figure 5. Optical micrographs taken between crossed polarizers of (a) 0.25:1.0 wt % SWNT−HA and (b) 0.50:1.0 wt % SWNT−HA dispersions taken immediately after sonication, no birefringence domains are visible; (c) 0.25:1.0 wt % SWNT−HA, the birefringence domains are visible; (d) 0.5:1.0 wt % SWNT−HA, the birefringence domains have increased and appear to have coalesced. Micrographs c and d were taken 8 h after sonication (scale bar: 100 μm). The dispersions were sonicated for 60 min with a small ($\sim$25 μL) droplet of the resulting dispersion placed between two glass coverslips followed by optical image analysis.

evolution of the phase boundary is observed at longer times, and this phase diagram can be considered to be at equilibrium.

The time taken for an isotropic dispersion to separate into a biphasic system was found to be dependent on the concentration of the SWNT−HA dispersion. The general trend appears to be that at a fixed concentration of HA the rate of phase separation increases as the SWNT concentration is increased. Two different SWNT−HA dispersions were compared immediately after sonication using optical microcopy taken between crossed polarizers (Figure 5, parts a and b) and again 8 h after sonication (Figure 5, parts c and d). The SWNT−HA dispersion depicted in the micrographs a and c in Figure 5 correspond to a ratio of 0.25:1.0 wt %, whereas micrographs b and d in Figure 5 correspond to 0.5:1.0 wt %. As stated above, immediately after sonication both dispersions were homogeneous and isotropic with no birefringent domains visible. At 8 h postsonication (Figure 5, parts c and d) both dispersions exhibited a biphasic system with birefringence visible. It is clear, however, that the proportion of the birefringence domains in micrograph d is greater than in c. This time dependence is also seen for HA, namely, when the SWNT concentration is fixed and the HA concentration increased of phase transition occurs more rapidly. These results indicate that it is possible to control the time of phase separation by either varying the SWNT or HA concentration while keeping the concentration of the other dispersion components fixed.

Many studies have shown that noncovalent functionalization of SWNTs by biological molecules facilitates[16,31,32] the debundling of SWNTs into homogeneous dispersions. By considering

(28) Grosberg, A.; Khokhlov, A. *Adv. Polym. Sci.* **1981**, *41*, 53.
(29) Savenko, S. V.; Dijkstra, M. *J. Chem. Phys.* **2006**, *124*, 234902.
(30) Dogic, Z.; Purdy, K. R.; Grelet, E.; Adams, M.; Fraden, S. *Phys. Rev. E* **2004**, *69*, 051702.
(31) Dalton, A. B.; Ortiz-Acevedo, A.; Zorbas, V.; Brunner, E.; Sampson, W. M.; Collins, L.; Razal, J. M.; Yoshida, M. M.; Baughman, R. H.; Draper, R. K.; Musselman, I. H.; Jose-Yacaman, M.; Dieckmann, G. R. *Adv. Funct. Mater.* **2004**, *14*, 1147.

the following experimental facts, (i) the nanotubes are not well dispersed at high HA concentration, (ii) nanotubes form a nematic phase at lower concentration when HA is added (Figure 4), and (iii) the rate of phase separation increases when HA is added, this phase separation behavior suggests that excess HA in solution induces attractive interactions between the nanotubes bundles. The exact nature of the attractive interaction is unknown; however, we suggest depletion interactions between the SWNTs mediated by the HA molecules in solutions as a possible mechanism. Depletion interactions have been observed in other CNT system stabilized using surfactants;[33−35] however, to date no literature has reported this interaction mechanism for SWNT systems stabilized with polymers or biological molecules. We propose that the extrapolation of the dashed line in Figure 4 to [HA] = 0 should correspond to the nanotube fraction needed to form a nematic phase in the absence of attractive interactions ($3.3D/L$). For example consider a weight fraction $f_w = 0.7$ wt % for the phase separation at [HA] = 0. If we assume a density of 1.3 g/cm^3 [16] for the nanotubes, this means that the volume fraction (f_v) is 0.54%. If we take $f_v = 3.3D/L$, this yields $D/L = 1.8 \times 10^{-3}$ ($L/D = 555$). This result is reasonable for thin bundles of nanotubes.

When HA is added, the phase transition is shifted toward lower nanotube concentrations. This is a case of a water-based nematic SWNT phase where the phase is simply controlled by varying the amount of dispersing additive. This allows the precise control of the system where the extent of phase separation can be chosen by the precise addition of a water-soluble biological molecule. In addition, attractive interactions allow the formation of nematic states at very low concentrations. Interestingly Rai et al.[18] and Davis et al.[19] also observed variations of the onset of phase separation by changing the nature of the superacids used as solvents. Their system involved the use of a mixture of acids to form superacids (102−123% H_2SO_4) to disperse the SWNTs which has to be performed in the absence of moisture. These superacid systems require careful handling in an anhydrous environment, whereby the system developed by us is water soluble and can be prepared at room temperature on a laboratory bench.

Typically for CNT systems avoiding or controlling the aggregation is difficult due to the strong van der Waals interactions between the tubes. We have observed that with dispersions formed from solutions where the SWNT is ≥0.5 wt % and the HA concentration is ≥1.0 wt % aging of the dispersion results in the continued evolution of nematic liquid crystal domains (Figure 6). These arise due to the coalescence of the nematic domains and result in the formation of larger nematic domains in equilibrium with the isotropic phase (Figure 6b).

Previous research has shown that CNT solutions can exhibit liquid crystalline ordering and rich rheological behavior, which is expected to depend on the tube or bundle aspect ratio. Sonication has been shown to affect the dimensions of SWNTs whereby long sonication times at high energy result in a decrease in length.[36] The spontaneous phase transition observed in the SWNT−HA system cannot be attributed to variations in the SWNTs aspect ratio from sample to sample as the dimensions of the SWNTs have been shown, using DLS and TEM, to be similar for various SWNT−HA samples (Table 1). This phase separation cannot be attributed to pH effects as all of the dispersions exhibited a pH between 6.2 and 6.4 regardless of whether the dispersion remained isotropic or underwent phase separation.

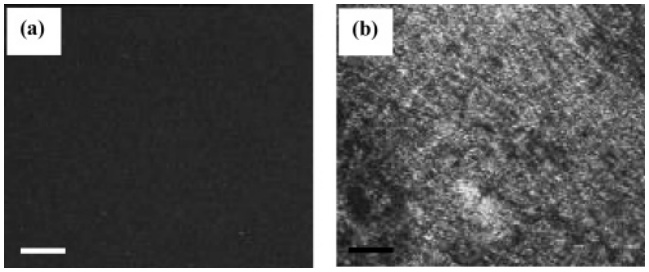

Figure 6. Optical micrographs of 0.5:1.0 wt % SWNT−HA dispersion taken between crossed polarizers (a) immediately after sonication and (b) 72 h after sonication (scale bar: 100 μm).

Table 1. Physical Characteristics of the SWNTs in Several SWNT−HA Dispersions[a]

SWNT−HA dispersion	0.1:0.1 wt %	0.5:0.5 wt %
average tube diameter (nm)[b]	1.20	1.20
average tube length (μm)[c]	1.22 (±0.03)	1.41 (±0.04)
aspect ratio[d]	1017 (±34)	1175 (±29)
phase property[e]	single-phase isotropic	biphasic

[a] The dispersions were prepared by sonicating the SWNT−HA solution for 60 min using a 13 mm step disruptor horn and a 3 mm tapered microtip, operating at a 20 kHz frequency. [b] The tube diameter was measured from TEM images taken from a diluted SWNT dispersion (ref 37). [c] The average tube length was determined using the DLS method (ref 36). [d] The aspect ratio was calculated by dividing the average tube length by average tube diameter. For the liquid crystal behavior we have to take into account the aspect ratio of the SWNT bundles. [e] The phase property was imaged 24 h after sonication.

It has been found that the change from isotropic to the biphasic organization is accompanied by an increase in viscosity (Figure 7). The initial isotropic dispersions all exhibited low viscosities; however, upon changing to a biphasic system the viscosity increased. It was apparent that as the degree of birefringence increased the viscosity of the dispersion increased to the point where the dispersion that exhibited the greatest birefringence (nematic liquid crystal) displayed gel-like characteristics. Viscosity measurements were performed at various stages after sonication with the measurements matched to the corresponding birefringent measurements (Figure 7). As the shear rate increased the viscosity of the dispersions decreases typical of a non-Newtonian fluid, and at all shear rates the viscosity of the dispersion increased with aging. It is clear from Figure 7 that as the dispersion aged the viscosity increased. As mentioned above, the phase separation displayed by the SWNT−HA dispersions occurs spontaneously at room temperature and upon aging. Therefore, in order to compare the characteristic viscosity for each dispersion we chose the viscosity value measured at a shear rate of 0.2 s^{-1}. This shear rate was chosen in order to eliminate any artificial viscosity variation

(32) Zorbas, V.; Ortiz-Acevedo, A.; Dalton, A. B.; Yoshida, M. M.; Dieckmann, G. R.; Draper, R. K.; Baughman, R. H.; Jose-Yacaman, M.; Musselman, I. H. *J. Am. Chem. Soc.* **2004**, *126*, 7222.
(33) Wang, H.; Zhou, W.; Ho, D. L.; Winey, K. I.; Fischer, J. E.; Glinka, C. J.; Hobbie, E. K. *Nano Lett.* **2004**, *4*, 1789.
(34) Islam, M. F.; Rojas, E.; Bergey, D. M.; Johnson, A. T.; Yodh, A. G. *Nano Lett.* **2003**, *3*, 269.
(35) Vigolo, B.; Coulon, C.; Maugey, M.; Zakri, C.; Poulin, P. *Science* **2005**, *309*, 920.
(36) Badaire, S.; Poulin, P.; Maugey, M.; Zakri, C. *Langmuir* **2004**, *20*, 10367.
(37) The TEM image is presented in the Supporting Information.

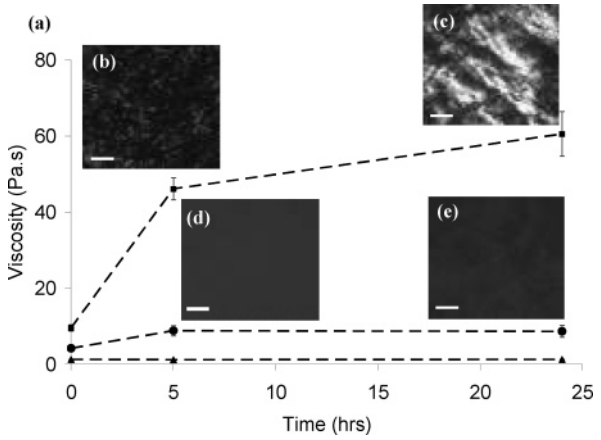

Figure 7. (a) Viscosity measurements of 0.5:0.5 wt % SWNT−HA (■), 0.25:0.25 wt % SWNT−HA (●), and 0.5 wt % HA (▲) (recorded at a shear rate of 0.2 s^{-1}) recorded at $t = 0$, 5, and 24 h after sonication, measured at 25 °C. The error bars represent the standard deviation obtained by measuring at least four different samples. The dispersions were sonicated for 60 min, then placed in an airtight vial and left to age for the designated time. The viscosities were recorded on a 0.250 mL aliquot of the respective dispersion. Optical micrographs of 0.5:0.5 wt % SWNT−HA (b and c) and 0.25:0.25 wt % (d and e) dispersion taken between crossed polarizers at 5 h (b and d) and 24 h (c and e) after sonication (scale bar: 100 μm).

due to applying a shear to the dispersion. A 0.5 wt % HA solution was also sonicated under identical conditions as the SWNT−HA dispersions and left to age for 24 h. The viscosity of the HA solution did not vary over the 24 h period and showed a lower viscosity value than the SWNT−HA dispersions.

Immediately after sonication ($t = 0$ in Figure 7a) both dispersions were isotropic exhibiting no birefringence. The variation in viscosities at $t = 0$ is due to the varying SWNT and HA concentrations in each dispersion. The increase in viscosity between 0, 5, and 24 h was greater for the more concentrated dispersion, and this greater viscosity matched the increase in the birefringence observed (Figure 7, parts b and c compared to parts d and e, respectively). That is to say the increase in viscosity was greater for the dispersion that exhibited SWNT liquid crystal nematic domains upon aging, namely, the 0.5:0.5 wt % SWNT−HA dispersion. The 0.25:0.25 wt % SWNT−HA dispersion exhibited no birefringence 5 or 24 h after sonication. The viscosity of the 0.25:0.25 wt % SWNT−HA dispersion increased slightly in the first 5 h, then remained constant. For this sample the attractive interaction (as indicated by the increase of viscosity) was not sufficient to induce a phase separation.

In summary, we have shown the slow but spontaneous phase separation of isotropic SWNT−HA dispersions into biphasic dispersions. This transition occurs upon standing at room temperature without any further addition of SWNTs to the dispersion. In addition, it is possible to tune the phase separation of the system by addition of the biological additive. These biphasic systems exhibited liquid crystalline nematic phases in equilibrium with the isotropic domains. Upon standing, the viscosity of the dispersion increased corresponding with the extent of birefringence arising from the formation of nematic phase domains. Further studies are currently taking place to elucidate the nature of the attractive interactions between the SWNTs and HA as well as the microenvironment surrounding the SWNTs during the phase separation process.

Acknowledgment. The authors acknowledge the Australian Research Council for their continued support and Dr. Weihua from the Faculty of Engineering at the University of Wollongong for support in obtaining the viscometry data. The authors also acknowledge Dr. Carol Lynam from the ARC Centre of Excellence for Electromaterials Science at the University of Wollongong for obtaining the TEM images. S.E.M. received financial support from A/Prof Donald Martin and OzNano2Life (CG060027), a project supported by the International Science Linkages program under the Australian Government's innovation statement Backing Australia's Ability.

Supporting Information Available: Experimental detail of the dynamic light scattering (DLS) method. TEM image of the HiPco SWNT. This material is available free of charge via the Internet at http://pubs.acs.org.

JA072160H